

Research Report

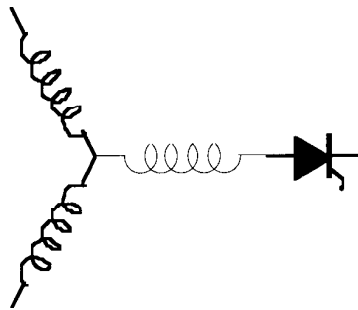
2001-10

**Adjustable-Speed Drive with Single-Phase Induction
Machine for HVAC Applications**

M. Chomat, T.A. Lipo*

Czech Academy of Sciences
Institute of Electrical Engineering
Prague, Czech Republic 182 02

*Wisconsin Power Electronic
Research Center
University of Wisconsin - Madison
Madison, WI 53703



**Wisconsin
Electric
Machines &
Power
Electronics
Consortium**

University of Wisconsin-Madison
College of Engineering
Wisconsin Power Electronics Research Center
2559D Engineering Hall
1415 Engineering Drive
Madison WI 53706-1691

© 2001 Confidential

Adjustable-Speed Drive with Single-Phase Induction Machine for HVAC Applications

Miroslav Chomat, *Member, IEEE*
Institute of Electrical Engineering
Czech Academy of Sciences
Dolejskova 5, 182 02 Prague
Czech Republic

Thomas A. Lipo, *Fellow, IEEE*
Department of Electrical and Computer Engineering
University of Wisconsin-Madison
1415 Engineering Drive
Madison, WI 53706, USA

Abstract--A novel low-cost drive with a single-phase induction machine for HVAC applications that require adjustable-speed operation is proposed. An experimental drive based on the proposed setup has been developed and built to verify its practical viability and properties. The paper presents results of investigation obtained by means of numerical simulations as well as experiments and discusses the properties and characteristics of the drive.

I. INTRODUCTION

Heating, ventilation, and air condition (HVAC) account for significant percentage of electric energy consumed especially in residential areas. Most of these applications utilize single-phase induction machines for driving fans and compressors. Increase in the energy efficiency of these devices of up to 30 % could be achieved by introduction of adjustable or multi-speed drives [1-3]. Continuing decrease in prices of current semiconductor components makes this solution more commercially viable and attractive.

A three-phase induction machine drive represents nowadays a standard solution for an adjustable-speed drive. Single-phase induction machines, however, still have a certain cost advantage over three-phase induction machines of comparable power due to higher production volumes, which is particularly true in the USA. This is one of the reasons why much attention is paid to variable-speed operation of single-phase machines. Most of these machines are of permanent split capacitor type with two phase windings of generally different parameters. It is, therefore, relatively straightforward to supply such machines with variable-frequency voltage from two or three-phase inverters [4-6].

This paper deals with another drive setup where a single-phase inverter is employed. The presented solution introduces a new low-cost drive utilizing a single-phase induction machine with speed control capability suitable for a great deal of HVAC applications. The proposed drive is specifically aimed at applications that do not have high demands on dynamic properties of the drive.

II. SYSTEM DESCRIPTION

The scheme of the system under investigation is shown in Fig. 1. The drive consists of a voltage doubler followed by a one-phase inverter with two MOSFET or IGBT switches. The drive is designed to run primarily in two modes of operation. In the full-speed mode, the main winding of the motor is fed with sinusoidal voltage supplied directly from the mains and the single phase PWM inverter generates a voltage waveform with suitable magnitude and phase shift in relation to the mains for the auxiliary winding. During reduced-speed operation, both windings are fed from the inverter. The phase shift between the currents in the main and auxiliary windings is then achieved by the connection of an AC capacitor of a proper value and rating in series with the auxiliary winding.

Such a configuration of the drive contains only two solid-state switches, which may be rated just for a fraction of the nominal power of the machine for a fan type load. This significantly reduces the overall losses in the semiconductor components and results in a smaller size of the heat sink and, therefore, of the whole drive, which may also help decrease manufacturing costs of the final product. The proposed design can also improve the reliability of the drive by enabling temporary operation with the supply of the motor directly from the mains in the case of an inverter failure. This would, however, require use of an AC capacitor with an increased voltage rating.

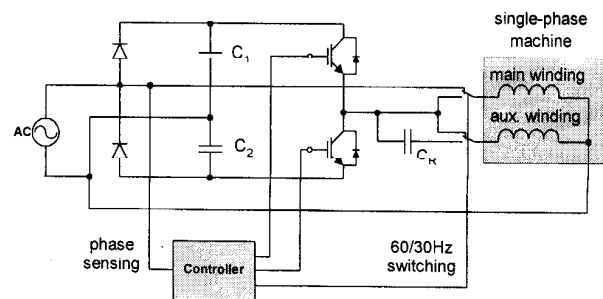


Fig. 1. Scheme of system under investigation.

III. NUMERICAL MODELING AND SIMULATIONS

The properties of the proposed drive setup were first analyzed by means of numerical simulation. The parameters of a practical 3/4 hp machine from an existing blower were used. The main parameters of the machine are in Table I. A supply voltage of 220 V_{RMS} at the input of the drive was considered. A steady-state mathematical model was used to determine the operating points of the machine under various working conditions and to calculate the optimal setting of the drive.

TABLE I
MOTOR RATING AND PARAMETERS

Power:	¾ h.p.	$R_{1m} = 9 \Omega$
Voltage:	230 V	$R_{1a} = 22 \Omega$
Frequency:	60 Hz	$R_2 = 10 \Omega$
Speed:	1110 rpm	$L_{1m} = 360 \text{ mH}$
Aux/Main turns ratio:	1.37	$L_{1a} = 700 \text{ mH}$
Run capacitor:	10 μF	

The optimal value of capacitance of the run capacitor was calculated for the considered machine. For such capacitance, maximal ratio between forward and backward rotating magnetic fields is achieved in the machine. The dependences of this value on slip for supply frequencies of 60 Hz and 30 Hz are plotted in Fig. 2. The optimal capacitance for normal 60 Hz operation would be 10 μF , which agrees with the value recommended by the manufacturer, and for 30 Hz operation, a capacitor of 30 μF would be needed.

First, standard operation of the machine with a run capacitor of 10 μF , for which the motor was originally designed, was simulated to obtain a reference for the assessment of the quality of the proposed drive setup. The machine was fed with a supply voltage of 220 V and 60 Hz. Fig. 3. shows the torque-speed characteristics, where the solid line denoted T_e represents the resulting electromagnetic torque of the machine and the dotted line denoted T_r shows the amplitude of the torque pulsations caused by unbalanced

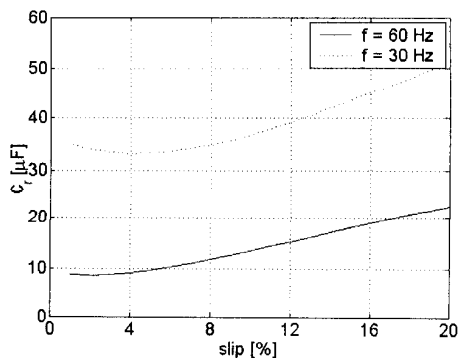


Fig. 2. Optimal run-capacitor capacitance.

voltage supply of the motor. The dashed line depicts the considered fan load torque-speed characteristic where $T_L \approx n^2$. Fig. 4 then shows the dependences of the current magnitudes in the main, I_m , and the auxiliary, I_a , windings.

Second, full-speed operation was investigated. The inverter supplying the auxiliary winding was controlled so that it generated a voltage of the same amplitude but shifted by 86° from the phase of the mains to achieve phase quadrature of the currents. The difference from voltage quadrature is given by the fact that the ratios between the real and imaginary parts of the impedances in the main and auxiliary windings are not equal to each other. The optimal phase angle between the voltages across the main and auxiliary windings was analytically determined based on the double revolving field theory, c.g. [7], from the parameters of the main and auxiliary windings in the considered machine so that the produced torque pulsations were minimized for the nominal speed.

Fig. 5 shows the torque-speed characteristics of the drive in the full-speed mode. It can be noted that the machine has quite high starting torque when fed in this manner. The relatively high value of the torque ripple near the nominal speed is mainly due to the limitation of the voltage amplitude generated by the inverter. Ideally balanced operation would require the magnitude of the voltage for the auxiliary winding to be approximately 30% above the magnitude of the voltage supplying the main winding for this particular machine. This is, however, not achievable with the considered front-end part of the converter and the employed PWM method. The

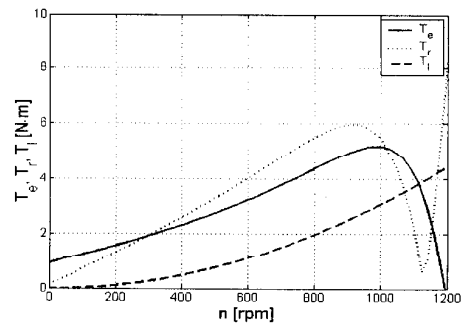


Fig. 3. Torque-speed characteristics, standard operation.

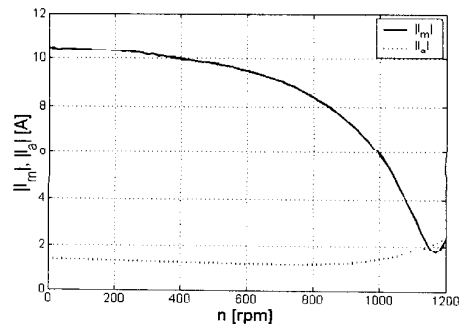


Fig. 4. Stator currents-speed characteristics, standard operation.

dependences of the magnitudes of currents in the main and auxiliary windings on the mechanical speed are presented in Fig. 6. It can be seen that the current in the auxiliary winding is significantly lower over the range of speed considered here implying a relatively low rating of the inverter.

Comparison of Figs. 5 and 6 with Figs. 3 and 4 reveals that the proposed drive setup provides in the full-speed mode significantly higher starting as well as breakdown torques than the permanent split capacitor motor. On the other hand, the produced torque ripple is higher for the proposed setup. The stator currents are comparable in both cases for the nominal operating speed.

Third, operation at a reduced speed was analyzed during which the inverter was producing a voltage waveform with amplitude of $110 V_{RMS}$ and a frequency of 30 Hz. A capacitor of $30 \mu F$ was connected in series with the auxiliary winding. The value of the capacitor was chosen to be optimal for the 30 Hz supply. The torque-speed characteristic and the dependence of the torque ripple on speed are in Fig. 7. The value of the torque pulsations has now a local minimum near the expected operating point. Fig. 8 shows the currents in the main and auxiliary windings together with the overall current drawn from the inverter, I_s . It can be noted that the amplitude of the current supplied by the inverter is similar in both cases. The magnitude of the AC voltage across the capacitor plotted against the speed is in Fig. 9.

Despite the fact that the capacitor is chosen to give best results at one particular supply frequency, it is possible to feed the machine in the reduced-speed mode with frequencies in a certain range around the optimal frequency. In our case, we have chosen 30 Hz as the optimal reduced-speed supply frequency corresponding to the $30 \mu F$ capacitor. Figs. 10 and 11 show the results of simulation when the machine is consecutively run at 18, 30, and 42 Hz, followed by the full-speed mode at 60 Hz. The load-torque characteristic of a fan from Fig. 3 was considered. It can be noted in Fig. 10 that the torque pulsations are significantly higher for 18 Hz and particularly for 42 Hz than for 30 Hz supply. This would not, however, represent any serious problem for most fan type load applications.

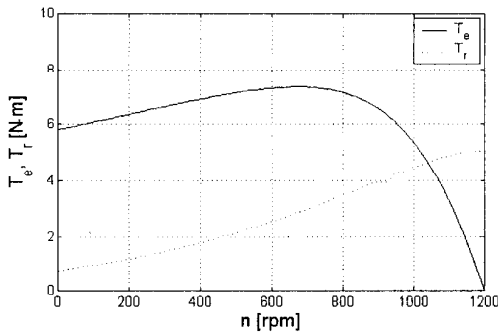


Fig. 5. Torque-speed characteristics, $f = 60$ Hz.

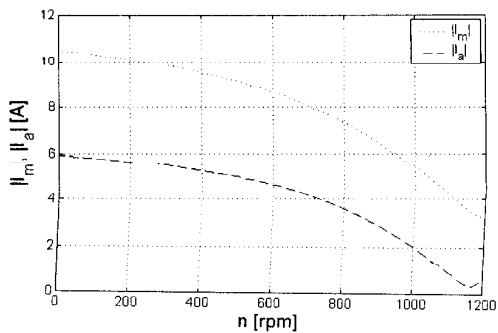


Fig. 6. Stator currents-speed characteristics, $f = 60$ Hz.

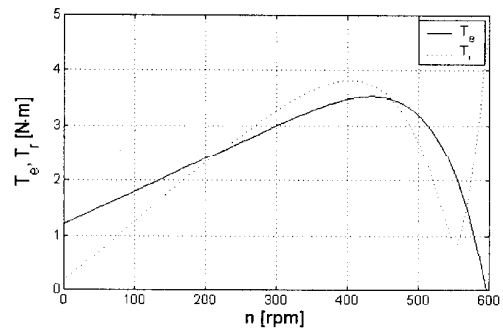


Fig. 7. Torque-speed characteristics, $f = 30$ Hz.

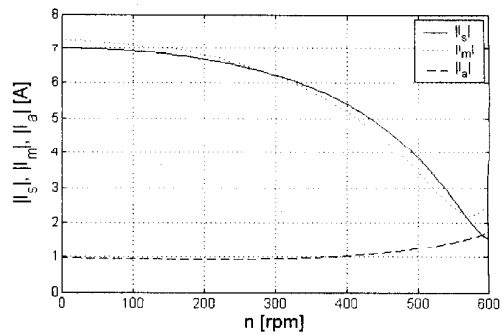


Fig. 8. Stator currents-speed characteristics, $f = 30$ Hz.

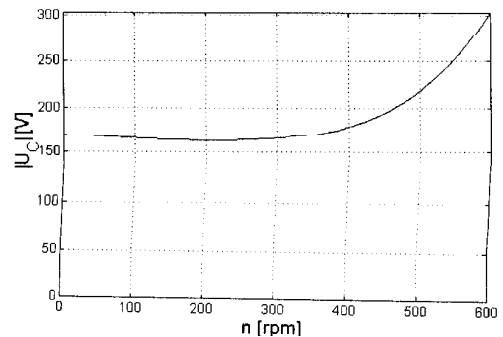


Fig. 9. Voltage across AC capacitor, $f = 30$ Hz.

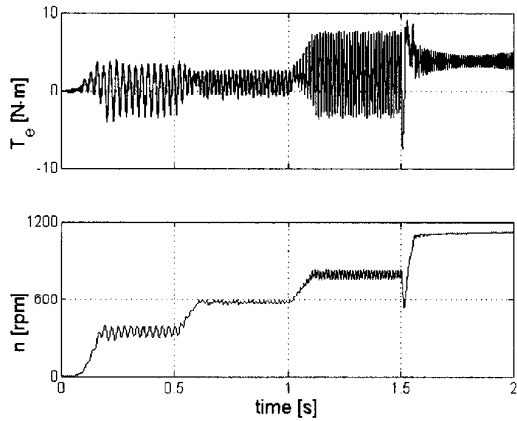


Fig. 10 Torque and speed during control of drive.

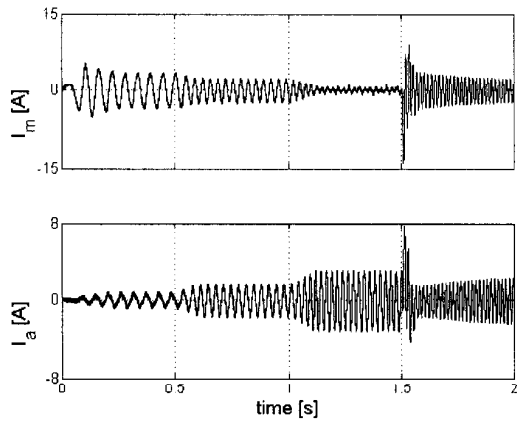


Fig. 11 Stator currents during control of drive.

IV. EXPERIMENTAL RESULTS

An experimental drive has been developed in order to verify the theoretical results and the practical viability of the proposed setup. The control algorithm was implemented in a control board based on a digital signal processor TMS320C240. The algorithm generated a PWM voltage waveform with variable amplitude and frequency with the possibility to synchronize the output with the line voltage. A set of measurements has been carried out in order to verify the theoretical results and analyze the behavior of the practical drive. Operation both at full speed (60 Hz) and at reduced speeds has been tested for different load torques.

The results for the full-speed operation are presented first. To take the different numbers of turns in the main and auxiliary windings into account, the currents in the auxiliary winding are multiplied by the proper turns ratio and correspond, therefore, rather to current layers in the machine. The plotted trajectory then directly indicates the quality of the supply voltage for the motor. Fig. 12 shows the shape of the

stator current layer for the full-speed operation when the phase shift between the voltages fed to the main and auxiliary windings is 90° . The motor connected to a dynamometer and loaded by 270 W rotated at 923 rpm. The current layer forms an ellipse with an angular deviation of the main axis from the real axis of the reference frame. It means that the angle between the currents in the main and auxiliary windings is different from the optimal 90° , which is caused by different impedances of the main and auxiliary windings.

Operation of the drive at half speed is illustrated in Figs. 13 and 14. An AC capacitor of $30 \mu\text{F}$ was used as a motor-run capacitor. The mechanical speed was 527 rpm and the load was 65 W. Fig. 14 shows the supply voltages at the stator windings terminals. It should be noted that the voltage stress for the auxiliary windings increased significantly in this mode of operation.

In general, switching between reduced-speed and full-speed modes may cause a transient response notable both in torque or speed and in stator currents of the machine. There are several methods available to keep these effects within some predetermined limits. Probably the ideal way would be to use exact timing of switching which would

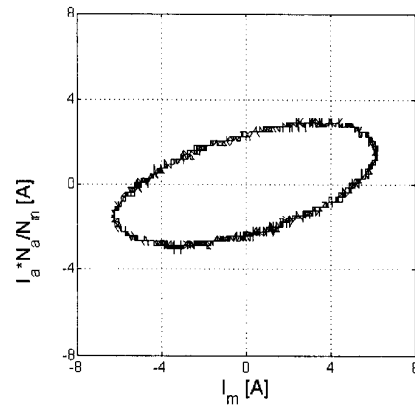


Fig. 12 Measured stator current layer, $f = 60 \text{ Hz}$, $\phi = 0^\circ$.

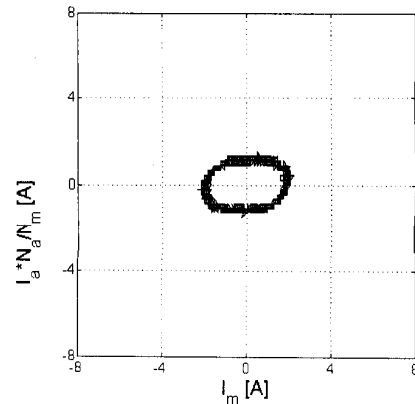


Fig. 13 Measured stator current layer, $f = 30 \text{ Hz}$, $C = 30 \mu\text{F}$.

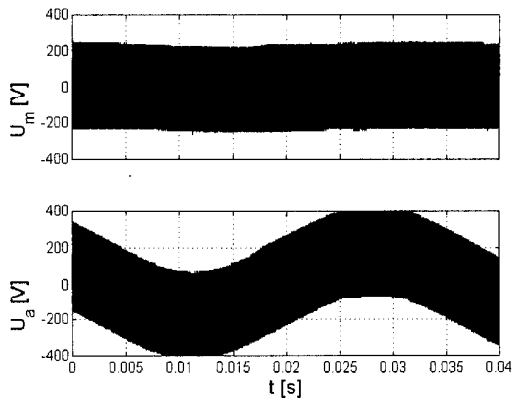


Fig. 14. Stator voltages, $f = 30$ Hz, $C = 30$ μ F.

minimize the transients and consume the minimal time. This is, however, not practical in the case of a low-cost and low-power drive. In our case, intermediate time intervals have simply been inserted during which the currents are allowed to decrease before applying the supply voltage of different frequency. This is shown in Figs. 15 and 16. The current in the main winding is in trace 1 and the current in the auxiliary winding in trace 2. Fig. 15 illustrates the transition from the full-speed in interval A to half-speed operation in interval D. Within interval B only the main winding is connected to the mains while the inverter is idle and the currents may flow only through the flywheel diodes of the inverter. In interval C both windings are disconnected and the current transient in auxiliary winding excited by disconnecting the main winding has enough time to decay. A similar approach, but in reverse order, is applied for the transition from half-speed to full-speed operation in Fig. 16. The entire transition process is synchronized with the phase of the supply voltage. In case the drive is connected to a load with relatively high moment of inertia, precautions need to be taken in order to maintain the DC-link voltage within some safety limits during braking.

V. CONCLUSIONS

The theoretical and experimental results have proven viability of the proposed drive setup and feasibility of its use for fan type HVAC applications in which the load torque varies with the square of speed. The drive represents a low-cost solution how to increase the energy efficiency of an HVAC application. It enables the device to operate with lower output by controlling the speed allowing, therefore, for significant gain in energy efficiency in comparison to mechanical regulation by outlet damper with fixed-speed drives. The presented solution minimizes also the number of semiconductor switches used in the inverter. The tests have shown that the “nonideal” supply of the machine in some modes of operation does not impair the practical operation of the drive.

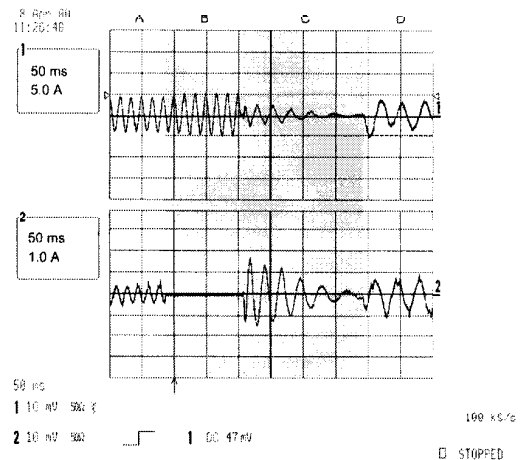


Fig. 15. Measured stator currents during transition from full to half-speed operation.

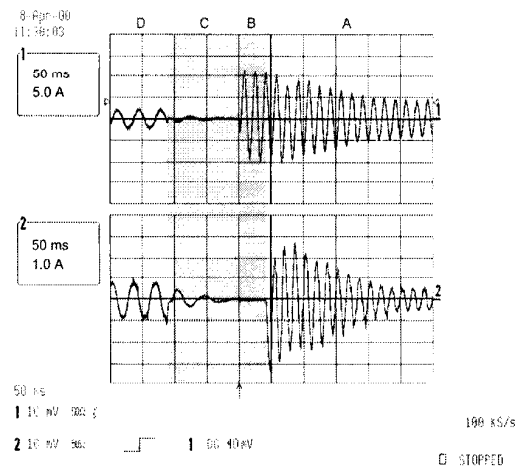


Fig. 16. Measured stator currents during transition from half to full-speed operation.

ACKNOWLEDGMENT

This work was supported by the National Science Foundation under Award Number 9820434 and by the Ministry of Education, Youth, and Sport of the Czech Republic under research grant ME332.

REFERENCES

- [1] H. N. Hickok, “Adjustable speed – a tool for saving energy losses in pumps, fans, blowers, and compressors,” *IEEE Trans. on Industry Applications*, vol. 21, pp. 124-136, January/February 1985.
- [2] N. P. van der Duijn Schouten, B. M. Gordon, R. A. McMahon, M. S. Boger, “Integrated drives as single-phase motor replacement,” in *Conference Record IEEE/IAS Annual Meeting*, pp. 922-928, 1999.
- [3] M. B. R. Correa, C. B. Jacobina, A. M. N. Lima, E. R. C. da Silva, “Single-phase induction motor drives systems,” in *Conference Record IEEE/APEC*, vol. 1, pp. 403-409, 1999.
- [4] E. R. Benedict, T. A. Lipo, “Improved PWM modulation for a permanent-split capacitor motor,” in *Conference Record IEEE Industry Applications Conference*, pp. 2004-2010, 2000.

- [5] A. L. Julian, R. S. Wallace, P. K. Sood, "Multi-speed control of single-phase induction motors for blower applications," *IEEE Trans. on Power Electronics*, vol. 10, no. 1, pp. 72-77, January 1995.
- [6] E. R. Collins, "Torque and slip behavior of single-phase induction motors driven from variable-frequency supplies," *IEEE Trans. on Industry Applications*, vol. 28, no. 3, pp. 710-715, May/June 1992.
- [7] P. C. Krause, O. Wasynczuk, S. D. Sudhoff, *Analysis of electric machinery*, New York: IEEE Press, 1995.